The Abdus Salam
International Centre for Theoretical Physics

United Nations
Educational, Scientific and
Cultural Organization

IAEA
International Atomic Energy Agency

2163-30

College on Soil Physics: Soil Physical Properties and Processes under Climate Change

30 August - 10 September, 2010

Average sand particle trajectory examined by the raindrop detachment and wind-driven transport (RD-WDT) process

Gunay Erpul
University of Ankara
Turkey

EARTH SURFACE PROCESSES AND LANDFORMS
Earth Surf. Process. Landforms (2009)

Published online in Wiley InterScience
(www.interscience.wiley.com) DOI: 10.1002/esp.1814

Average sand particle trajectory examined by the Raindrop Detachment and Wind-driven Transport (RD-WDT) process

G. Erpul,[1]* D. Gabriels,[2] W. M. Cornelis,[2] H. Samray[1] and T. Guzelordu[1]
[1] Department of Soil Science, Faculty of Agriculture, University of Ankara, 06110 Diskapi-Ankara, Turkey
[2] Department of Soil Management and Soil Care, Ghent University, Coupure Links 653, B 9000 Ghent, Belgium

Received 1 September 2008; Revised 26 December 2008; Accepted 24 February 2009

* Correspondence to: G. Erpul, Department of Soil Science, Faculty of Agriculture, University of Ankara, 06110 Diskapi-Ankara, Turkey. E-mail: erpul@agri.ankara.edu.tr

ESPL
Earth Surface Processes and Landforms

ABSTRACT: Recent studies of soil loss by the integrated action of raindrop impact and wind transport have demonstrated the significance of this mechanism. This paper presents data obtained during wind-tunnel experiments examining the 'Raindrop Detachment and Wind-driven Transport' (RD-WDT) process to investigate average sand particle trajectory and the spatial extent at which the process operates. In the experimental design, at the same time as the horizontal wind velocities of 6·4, 10, and 12 m s^{-1} passed through the tunnel, rainfall was simulated falling on very well sorted dune sand. The aspect and slope of the sand bed was varied to reproduce both windward (Ww) and leeward (Lw) slopes of 4° and 9° with respect to the prevailing wind direction. The average sand particle trajectories by the RD-WDT process ($\bar{X}_{RD-WDT}$) were estimated by a mass-distribution function, which was integrated over a 7-m uniform slope segment. The results showed that $\bar{X}_{RD-WDT}$ depended statistically upon the wind shear velocity (u^*), and the effect of the slope gradient (θ) was insignificant on $\bar{X}_{RD-WDT}$. This was different from that of the windless rain process ($\bar{X}_{RD-ST}$), 'Raindrop Detachment and Splash-driven Transport' (RD-ST), the spatial range of which relies strongly on θ. Additionally, $\bar{X}_{RD-WDT}$ was approximately 2·27 ± 2·2 times greater than the average path of a typical saltating sand particle of the rainless wind ($\bar{X}_{WZ-ST}$), 'Wind Erosion Saltation Transport' (WE-ST). Copyright © 2009 John Wiley & Sons, Ltd.

KEYWORDS: sand particle trajectory; wind-driven rain; rainsplash; saltation

Introduction

Studies of wind-driven rain erosion processes have considerably improved the prediction of soil loss by the integrated action of raindrop impact and wind transport (Erpul and Gabriels, 2006). For example, when rainsplash and saltation sub-processes are considered, Erpul *et al*. (2004) reports that the process of 'Raindrop Detachment and Wind-driven Transport' (RD-WDT) under wind-driven rain differs from those under rain-free wind and wind-free rain. Rainsplash erosion alone [Raindrop Detachment and Splash Transport (RD-ST)] (Kinnell, 1999, 2005) is considered as a transport limited system since transporting agents are not strong enough to carry detached particles. The principal role of splash action by raindrop impact is therefore in the detachment of soil particles prior to their removal by existing agents such as overland flow, concentrated flow or wind (Morgan, 2007). However, in saltation, a grain that is small enough to be lifted but not small enough to stay in the air current is transported by rain-free wind. Of the three modes of aeolian particle motion, creep (>500 m), saltation (50–500 m) and suspension (<100 m) (Bagnold, 1941), a saltation mode [Wind Erosion Saltation Transport (WE-ST)] is the first requirement in any description of aeolian transport processes (Gillette, 1977; Shao *et al.*, 1993; Raupach and Lu, 2004). Saltation is a transport limited system if the supply of sand particles at the surface is infinite (Bagnold, 1941; Raupach and Lu, 2004). In this system, the ejected grain falls back bombarding the surface with high energy (Gillette, 1977; Shao *et al.*, 1993) and initiating the movement of other particles.

The RD-WDT process differs from the WE-ST process of rainless wind because, rather than sand bombardment causing particle detachment, raindrops hitting the surface initiate the jumping movement of sand particles, which are subsequently transported by wind. In addition to its role in particle transport, wind changes the velocity, frequency, and angle of the raindrop impact and significantly affects the rainsplash detachment rate or dislodgement rate, too (Erpul *et al.*, 2003a). Unquestionably, the RD-WDT process differs from the RD-ST process of windless rain in a way that raindrops impacting the surface set off the jumping movement of sand particles and afterward the slope gradient determines the distance the sand particle travels rather than the wind (Riezebos and Epema, 1985; Wright, 1986, 1987; Poesen, 1985).

The RD-WDT process could clearly contribute to soil loss during storm events when intense rains and strong winds work together (Pedersen and Hasholt, 1995; Erpul, 2001; Erpul *et al.*, 2003b). Goossens *et al.* (2000) reported that spatial variations

in rainfall during rain events were the major cause of the differences in splash drift over a field, and that wind caused oblique rainfall and an extra-displacement of soil particles in the downwind direction. Vieira *et al*. (2004) presented the influence of oblique rainfall on the genesis of coarse sand accumulations and emphasized the importance of RD-WDT as a main transportation mechanism. The importance of the process on blanket peat erosion was signified by Warburton (2003), Evans and Warburton (2005) and Foulds and Warburton (2007a). Foulds and Warburton (2007b) found that dust flux rates by saltation were in general up to two-orders of magnitude lower than that recorded during periods of sustained wet weather. Their measurements verified the previously unreported rapid switch in process regime between wind-driven rainfall and dry blow deflation in blanket peat environments. Distinction of the climatic variables for the cases of either rain-free wind and wind-free rain or wind-driven rain cases is significant for modeling the sub-processes of wind and water erosion at a large range of spatial and temporal scales (Visser and Palma, 2004). For instance, Visser and Sterk (2007) stated that either uphill or downhill transport of sediments could occur by RD-WDT, depending upon the prevailing wind direction unlike the downhill only movement of particles by RD-ST. Erpul *et al*. (2003b) showed that the sediment transport from interrill areas was under-predicted considerably when the contribution of the RD-WDT process to the interrill erosion could not be accounted for, which suggests that RD-WDT should accurately be represented in the prediction models for water erosion under wind-driven rain.

The current paper investigates the average sand particle trajectory by RD-WDT ($\bar{X}_{RD-WDT}$), being particularly related to the extent at which the process spatially acts, and aims to improve the understanding of this transport process by the integrated action of raindrop impact and wind transport.

Material and Methods

The RD-WDT experiments were performed under laboratory conditions in the wind tunnel rainfall simulator facility of the International Center for Eremology (ICE), Ghent University, Belgium. The details of the wind tunnel were given by Gabriels *et al*. (1997), and it was complementarily detailed by Cornelis *et al*. (2004a), additionally including particulars of the drop size distribution, intensity, and energy of the wind-driven rains of the wind tunnel simulator. In the study, a continuous spraying system of 10 downward-oriented nozzles simulated rainfall at the same time as the horizontal wind velocities of 6·4, 10, and 12 m s^{-1} were generated. Tap water was used with an electrical conductivity of 0·7 dS m^{-1} at 25 C since dispersion could be ignored. The raindrop size distributions for wind-driven rains in the facility were described in detail by Erpul (1996) and Erpul *et al*. (1998, 2000). In general, the raindrop sizes of wind-driven rains have a narrow range around the median raindrop size, and the most dominant raindrop size is 1·8 mm. Table I shows the resultant impact velocities and the kinetic energies of wind-driven rains measured by the kinetic energy sensor (Erpul *et al*., 2003a).

Table I. Summary of the raindrop impact velocities and kinetic energies as functions of horizontal wind velocities for 1·8 mm raindrop size (Erpul *et al*., 2003a)

u (m s^{-1})	v (m s^{-1})	KE (J)
6·4	4·64	$2{\cdot}47 \times 10^{-5}$
10·0	5·51	$5{\cdot}51 \times 10^{-5}$
12·0	10·48	$1{\cdot}07 \times 10^{-4}$

Note: u, horizontal wind velocity; v, resultant raindrop impact velocity; KE, kinetic energy.

The wind-driven rainfall intensities intercepted by windward (Ww) and leeward slopes (Lw) of 7% and 16% (4·0 and 9·0 , respectively) varied with the angle of the rain incidence during the simulations (Sharon, 1970, 1980; Sharon *et al*., 1983; Sharon *et al*., 1988; De Lima, 1990; Sharon and Arazi, 1997; Blocken and Carmeliet, 2000, 2002, 2004; Blocken *et al*., 2005; Cornelis *et al*., 2004a; Blocken *et al*., 2006) and are given in Table II. There were significant differences in the wind-driven rainfall intensities between Ww and Lw slopes. In previous studies, the impact frequency of raindrops with a given energy determined the sand detachment rate at which sand particles were supplied into the wind, but wind was the only factor that transported the particles over some distances. The RD-WDT in this study was a detachment-limited erosion system since the capacity of the wind currents was sufficient to transport detached sand particles.

Details of the experimental set-up which were specially designed for the wind-driven rain erosion studies have been reported by Erpul *et al*. (2002, 2004, 2008a, 2008b) (Figure 1). Not only the sand pan but also the whole false bottom of the wind tunnel was adjusted for the slopes of 4 and 9 to maintain streamlined air currents and avoid edge effects on the wind velocity profiles.

The sand used in this study was very well sorted dune sand with a geometric particle diameter of 250 m (Figure 2). Calcium carbonate and organic matter content were 3·34% and 0%, respectively. The electrical conductivity of the sand was 0·72 dS m^{-1} at 25 C and the bulk density was 1·7 Mg m^{-3} (Cornelis *et al*., 2004b, 2004c). The sand was placed into a 55-cm long and 20-cm wide pan with a perforated base to allow free drainage, and it was located at a distance x = 6·45 m downwind from the entrance of the wind tunnel working section (Figure 1a) along its centerline with both Ww and Lw slopes (Figure 1b and 1c, respectively) of 4 and 9 . For each run, the surface was pre-wetted by spraying before it was exposed

Table II. Variation of the wind-driven rainfall intensities with the rain incidence angle during the simulations

	Ww						Lw					
	6·4 m s^{-1}		10·0 m s^{-1}		12·0 m s^{-1}		6·4 m s^{-1}		10·0 m s^{-1}		12·0 m s^{-1}	
θ (deg)	M	SD	M	SD	M	SD	M	SD	M	SD	M	SD
4	130	6	139	18	148	19	106	5	98	13	95	12
9	145	7	166	22	181	23	91	5	72	10	62	8

Note: Ww, windward slope; Lw, leeward slope; u, horizontal wind velocity (in m s^{-1}); θ, slope gradient; M, mean wind-driven rainfall intensity (in mm h^{-1}); SD, standard deviation of the wind-driven rainfall intensity.

DOI: 10.1002/esp

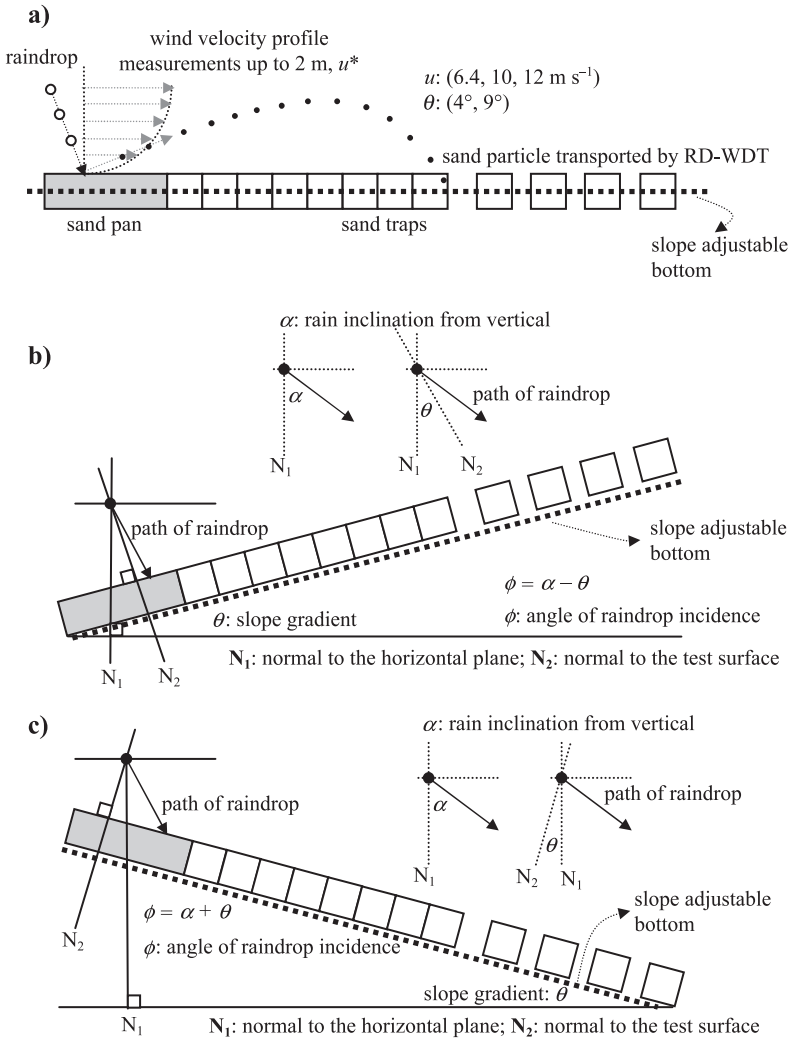

Figure 1. Experimental set-up with sand pan and traps for RD-WDT: (a) plan view, (b) side view of windward set-up, and (c) side view of leeward set-up.

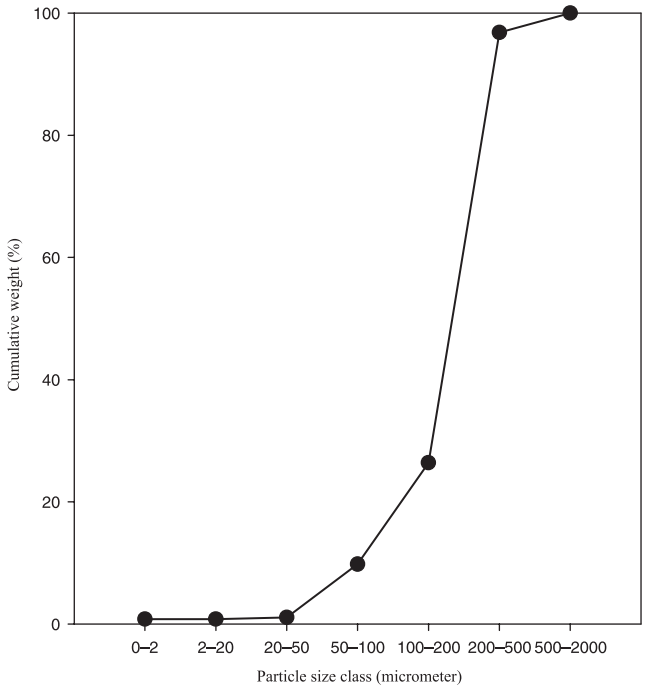

Figure 2. Cumulative grain size data of the sand used in the RD-WDT experiments.

to the wind-driven rain to prevent sand from lifting off due to wind, and smoothed exactly on a level with the rim of the pan. Accordingly, there was only raindrop-induced, no wind-induced, particle entrainment in the experiment. With three-wind velocities, two-slope gradients, two-slope aspects, and six replicates, a total of 72 wind-driven rainfall simulations were performed.

Wind velocity profiles were measured above the sand pan up to a 2 m nozzle height with a vane type anemometer and associated recording equipment (Figure 1a), and characterized by the Prandtl-von Kármán logarithmic equation:

$$u(z) = \frac{u^*}{\kappa} \ln \frac{z}{z_0} \quad \text{for } z < z_0 \tag{1}$$

where $u(z)$ is the wind speed at height z, z_0 is the aerodynamic roughness height, u^* is the wind shear velocity, and κ is the von Kármán's constant. The boundary layer was set at 0·3 m above the sand tray, and the resulted aerodynamic roughness height was 0·0006 m. Subsequently, using the exponential description of Equation 1, 'u^*' for 6·4, 10·0, and 12·0 m s^{-1} horizontal winds was derived (Table III). Average wind velocity profiles did not vary with the slope gradient but changed with the slope aspect since the experimental sets-up with a sand pan and traps for the RD-WDT changed with the slope aspect.

The value of $\bar{X}_{RD-WDT}$ was evaluated by the amount of wind-driven sand particles trapped at set distances on a 7-m

DOI: 10.1002/esp

Table III. Regression parameters of the exponential wind velocity profiles[a]

		Ww		Lw	
u (m s^{-1})	a	b	u^* (m s^{-1})	b	u^* (m s^{-1})
6·4	0·0006	0·75	0·53	1·18	0·34
10·0		0·62	0·65	0·77	0·52
12·0		0·53	0·76	0·65	0·62

[a] *Note*: $z = ae^{b(u)}$, where $a = z_0$ and $b = \kappa/u^*$ and $a = 0{\cdot}0006$ m. Ww, windward slope; Lw, leeward slope; u, horizontal wind velocity (in m s^{-1}).

uniform slope segment (Figure 1). The sand particles trapped in the collecting troughs were washed, oven-dried and weighed, and mass distribution of sand particles with travel distance (x, in meters) was acquired for each simulation. These were used to produce exponential decay curves, and exponentially fitted curves with parameter values (β and δ coefficients that depended upon the physical properties of the sand particles) were integrated over the RD-WDT distance to determine $\bar{X}_{\mathrm{RD-WDT}}$ (Equation 2) (Savat and Poesen, 1981; Poesen, 1985; van Dijk *et al.*, 2002; Wright, 1987; Mouzai and Bouhadef, 2003; Erpul *et al.*, 2003a, 2004; Legue'dois *et al.*, 2005; Legout *et al.*, 2005; Furbish *et al.*, 2007).

$$\bar{X}_{\mathrm{RD-WDT}} = \frac{1}{d-c}\int_c^d \beta e^{-\delta x}\partial x \tag{2}$$

Equation 2 gives an approximation of the average value of the mass distribution curves over the interval $c \le x \le d$, where the lower limit $c = 0$.

Results

Scatter plots of the mean values together with the error bars for the sand amounts trapped at set distances along the horizontal plane are presented in Figure 3, and the relevant parameters (β and δ) of these curves, which were exponentially fitted by Equation 3, are given in Table IV.

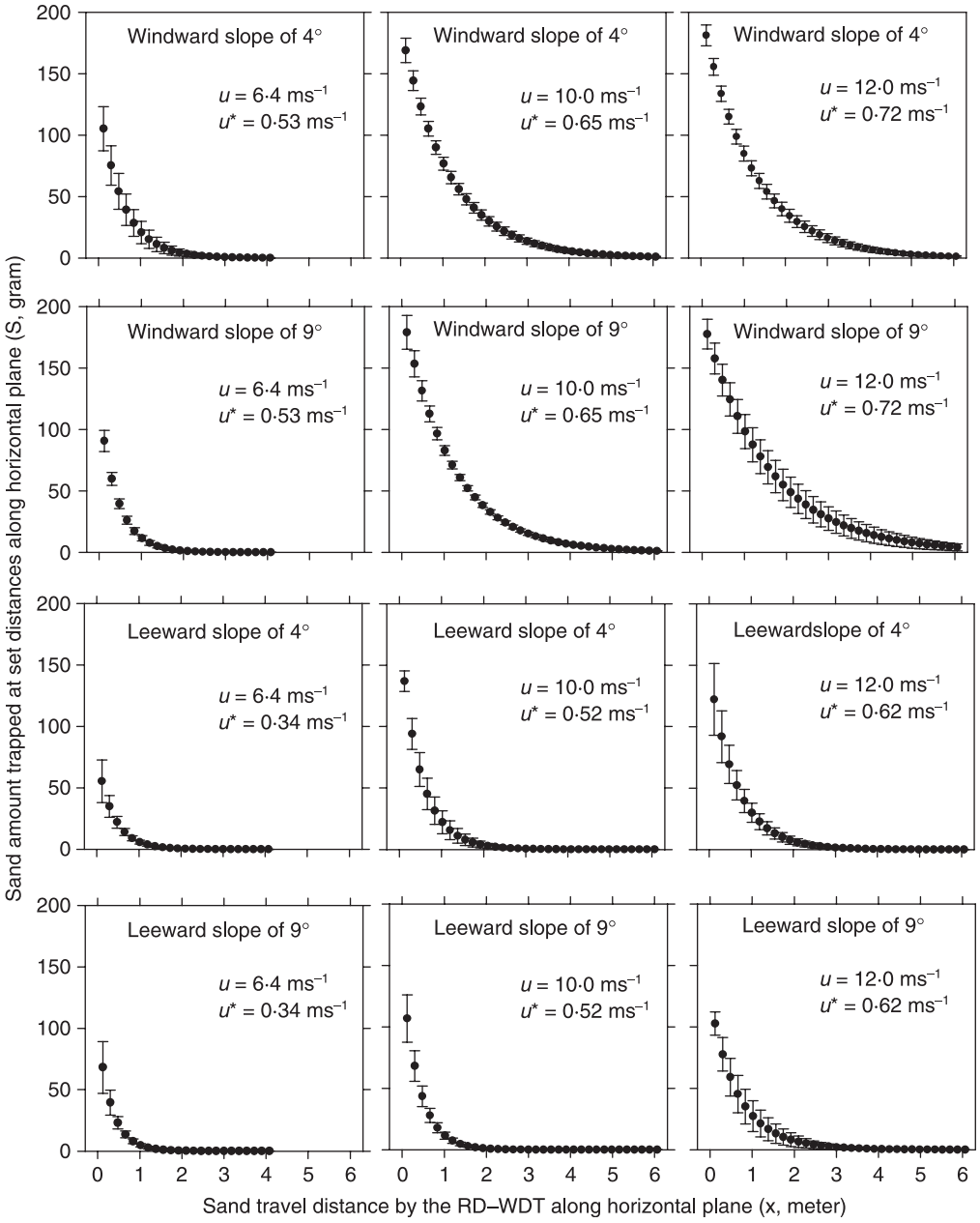

Figure 3. The mean sand amounts trapped at set distances on a 7-m uniform slope along the horizontal plane.

DOI: 10.1002/esp

Table IV. The β and δ values of the mass distribution curves exponentially fitted by Equation 3[a]

n	Ww												Lw									
	4						9						4				9					
	0·53		0·65		0·76		0·53		0·65		0·76		0·34		0·52		0·62		0·34		0·52		0·62	
	β	δ	β	δ	β	δ	β	δ	β	δ	β	δ	β	δ	β	δ	β	δ	β	δ	β	δ	β	δ
1	129	2·46	172	0·91	144	0·68	146	2·58	192	0·87	143	0·46	56	2·32	86	2·05	64	0·89	17	1·75	33	1·71	35	1·61
2	131	2·55	173	0·90	186	0·73	118	2·51	183	0·83	171	0·51	69	2·42	87	2·01	59	0·74	49	2·70	29	1·67	32	1·62
3	128	1·56	180	0·86	180	0·86	76	2·16	205	0·89	153	0·63	42	1·97	134	1·55	45	1·38	46	2·16	53	2·32	66	0·74
4	115	1·44	182	0·89	185	0·89	89	1·97	182	0·82	157	0·65	56	2·17	114	1·39	43	1·34	77	2·92	49	2·09	59	0·56
5	172	1·65	131	0·72	179	0·85	73	2·15	133	0·73	142	0·67	60	2·91	116	1·45	115	1·30	65	2·96	82	2·03	49	0·62
6	117	1·68	129	0·67	165	0·73	90	1·95	129	0·67	182	0·72	74	2·42	107	1·40	99	1·07	54	2·80	86	2·09	46	0·44
M	132	1·99	161	0·83	173	0·79	99	2·22	171	0·80	158	0·61	60	2·37	107	1·64	71	1·12	51	2·55	55	1·99	48	0·93
SD	21	0·48	24	0·10	16	0·09	28	0·27	32	0·08	16	0·10	11	0·32	18	0·31	30	0·26	20	0·49	24	0·25	13	0·54

Note: Ww, windward slope; Lw, leeward slope; u^*, wind shear velocity (in m s^{-1}); θ, slope gradient; *M*, mean; SD, standard deviation; *n*, replicate; β, the amount of sand trapped at the first trap (*y*-intercept of the mass distribution curve); δ, decay rate (the slope of the exponential function of Equation 3.

[a] The values of u^* are 0·53, 0·65, and 0·76 m s^{-1} at the Ww slopes and 0·34, 0·52, and 0·62 m s^{-1} at the Lw slopes for the horizontal wind velocities (u) of 6·4, 10·0, and 12·0 m s^{-1}, respectively.

$$S(x)_i = \beta e^{-\delta x_i} \tag{3}$$

where, S_i (gram) is the sand amount trapped at set distances (x_i, in meters) along the horizontal plane, and β and δ are the amount of sand trapped at the first trap (*y*-intercept of the mass distribution curve) and the decay rate (the slope of the exponential function), respectively.

The value of β was directly linked to the energy flux of the wind-driven rainfall (the raindrop energy multiplied by the raindrop impact frequency), indicating the magnitude of the sand detachment rate (Ellison, 1947; Heymann, 1967; Springer, 1976; Gilley *et al.*, 1985; Gilley and Finkner, 1985; Sharma and Gupta, 1989; Pedersen and Hasholt, 1995), which is outside the context of this present paper. Related works for the detachment rates by wind-driven raindrops are given in detail by Erpul (2001) and Erpul *et al.* (2003a, 2005, 2008a). However, the value of δ implicitly signified the effect of the transporting agent on the trajectory of the sand particles. From the values of δ, it was obvious that the decay rate of the mass distribution curves decreased with the increases in u^*, implying that the sand particles travelled longer distances as u^* increased (Table IV).

The mean values of $\bar{X}_{RD-WDT}$ calculated by Equation 2 are given in Table V for each θ and u^* for the Ww and Lw slopes.

The factorial analysis of variance (SAS, 1995) performed in order to examine the effect of u^* and θ on $\bar{X}_{RD-WDT}$ is given in Table VI for the Ww and Lw aspects. Statistical results showed that θ had no significant effect on $\bar{X}_{RD-WDT}$, and the effect of u^* was significant at $p = 0{\cdot}0001$ for both aspects. Two-way interactions of $\theta \times u^*$ also appeared statistically insignificant.

Furthermore, Pearson correlation coefficients separately evaluated for the Ww and Lw slopes are presented in Table VII. $\bar{X}_{RD-WDT}$ had the greatest correlation coefficient with u^* (0·94 and 0·89, respectively for the Ww and Lw slopes), indicating the significance of wind in predicting the average path of the sand particles travelled by the process of the RD-WDT. However, $\bar{X}_{RD-WDT}$ had very poor coefficients with θ (0·097 and 0·048, respectively for the Ww and Lw slopes). Conclusively, wind streams parallel to the surface did transport the detached sand particles under wind-driven rain, and evidently, θ had no significant role in determining the operational scale of the process. This finding confirmed an approach to the RD-WDT process that sand particles, once entrained into splash droplets, leave the surface with an initial lift-off velocity and angle and travel some distance, which varies directly with the wind velocity gradient (Rutin, 1983; De Lima, 1989; De Lima *et al.*, 1992; Jungerius and Dekker, 1990; Van Dijk *et al.*, 1996; Goossens *et al.*, 2000).

The value of $\bar{X}_{RD-WDT}$ is finally fitted into a simple linear regression model in the form of Equation 4 (Owen, 1980):

$$\bar{X}_{RD-WDT} = b_1 \frac{u^{*2}}{g} \tag{4}$$

where, b_1 is the slope term when the regression line passes through the origin, and u^{*2}/g shows the momentum loss per unit time per unit length per unit lateral dimension (Bagnold, 1941; Greeley and Iversen, 1985; Erpul *et al.*, 2002, 2004) for the sand particles transported by the RD-WDT process. The intercept term (b_0) is dropped from the linear regression model of a model $\bar{X}_{RD-WDT}$ with u^{*2}/g because b_0 is a parameter that shows the travel distance when $u^* = 0$, and representative of $\bar{X}_{RD-WDT}$ of windless rain and influenced only by θ (Moeyersons and De Ploey, 1976; Quansah, 1981; Poesen and Savat, 1981; Moeyersons, 1983; Grosh and Jarrett, 1994; Poesen, 1985, 1986; Wright, 1986, 1987; Kinnell, 2005; Furbish *et al.*, 2007), rather than $\bar{X}_{RD-WDT}$ (De Ploey, 1980;

DOI: 10.1002/esp

Table V. Variation of $\bar{X}_{RD-WDT}$ ws the slope gradient and the wind shear velocity at the windward and leeward slopes

	Ww						Lw					
	4°			9°			4°			9°		
n	0·53	0·65	0·76	0·53	0·65	0·76	0·34	0·52	0·62	0·34	0·52	0·62
1	0·53	0·98	1·16	0·61	1·11	1·36	0·45	0·43	1·03	0·50	0·66	1·09
2	0·51	0·90	1·20	0·62	1·11	1·28	0·53	0·52	1·00	0·42	0·66	1·12
3	0·65	1·09	1·18	0·55	1·15	1·28	0·43	0·61	0·96	0·53	0·66	1·05
4	0·70	1·08	1·18	0·60	1·15	1·37	0·49	0·72	1·09	0·43	0·71	0·98
5	0·72	1·11	1·21	0·55	1·10	1·27	0·36	0·64	0·93	0·43	0·62	0·97
6	0·71	1·15	1·31	0·71	1·15	1·38	0·55	0·69	1·15	0·43	0·73	1·02
M	0·64	1·05	1·21	0·61	1·04	1·32	0·47	0·60	1·02	0·46	0·67	1·04
SD	0·09	0·09	0·05	0·06	0·02	0·05	0·07	0·11	0·08	0·05	0·04	0·06

Note: Ww, windward slope; Lw, leeward slope; u^*, wind shear velocity (in m s^{-1}); θ, slope gradient; *M*, mean; SD, standard deviation; *n*, replicate.
[a] The values of u^* are 0·53, 0·65, and 0·76 m s^{-1} at the Ww slopes and 0·34, 0·52, and 0·62 m s^{-1} at the Lw slopes for the horizontal wind velocities (u) of 6·4, 10·0, and 12·0 m s^{-1}, respectively.

Table VI. Factorial analysis of variance of slope aspect, slope gradient, and wind shear velocity with $\bar{X}_{RD-WDT}$

Source	df	Ww			Lw		
		MSE	*F* value	*P* > *F*	MSE	*F* value	*P* > *F*
θ	1	0·027	3·07	0·0892	0·005	0·37	0·5493
u^*[a]	1	2·515	289·60	0·0001**	1·761	125·57	0·0001**
$\theta \times u^*$	1	0·033	3·76	0·0613	0·002	0·14	0·7084

Note: Ww, windward slope; Lw, leeward slope; u^*, wind shear velocity (in m s^{-1}); θ, slope gradient; df, degree of freedom; MSE, mean square error.
[a] The values of u^* are 0·53, 0·65, and 0·76 m s^{-1} at the Ww slopes and 0·34, 0·52, and 0·62 m s^{-1} at the Lw slopes for the horizontal wind velocities (u) of 6·4, 10·0, and 12·0 m s^{-1}, respectively.
** Statistically significant at the level of $p = 0{\cdot}05$.

Jungerius *et al.*, 1981; Rutin, 1983; Jungerius and Dekker, 1990; De Lima *et al.*, 1992; Erpul *et al.*, 2002, 2004; Cornelis *et al.*, 2004b; Cornelis *et al.*, 2004c) and there were no windless rain tests.

Linear regression models with $b_0 = 0$ for predicting $\bar{X}_{RD-WDT}$ by u^{*2}/g for the Ww and Lw slopes of 4 and 9 are given in Figures 4(a)–4(d), respectively. The values of b_1 were approximately 22·0 and 22·8 for the Ww slopes of 4 and 9 , respectively (Figures 4a and 4b), and those of the Lw slopes were 25·5 and 26·6, respectively (Figures 4c and 4d). For all data irrespective of the slope gradients and aspects, the statistical fit of this function is shown in Figure 4(e). The result showed that b_1 is equal to $23{\cdot}4 \pm 2{\cdot}18$ for all data collected in the study, and b_1 is approximately 2·27 (= 23·4/10·3) times greater than $\bar{X}_{WE-ST}$ (White and Schulz, 1977; Owen, 1980).

Discussion

To understand the differences of the RD-WDT process from the RD-ST and WE-ST processes, it is important to acquire knowledge on what forces affect the initial vertical velocity of particle lift-off and how the distance traveled by a particle depends on the wind velocity profile.

By the numerical studies of raindrop impact on both rigid case and elastic deformation case, Huang *et al.* (1982, 1983) in detail explained the rainsplash phenomena. They showed that the magnitude of the lateral shear stress of a vertically impacting raindrop was straightforwardly correlated to that of the compressive stress, and Al-Durrah and Bradford (1982) described how compressive stress was transformed to or compensated by lateral shear stress from the radial splashes. This compensation is affected by θ, for example Wright (1986) and Poesen (1985) emphasized the effects of θ on the direction and magnitude of the splash asymmetry. When more momentum is transferred in the downslope direction, the difference between upslope and downslope travel distances increases. Nearing *et al.* (1986) calculated average pressures under impact from the force measurements and an approximation of water drop contact area as a function of time. They reported that the compressional wave generated in the water upon impact is probably an important parameter in determining the level and time distribution of forces during impact.

Table VII. Pearson correlation coefficients among slope gradient, wind shear velocity, and $\bar{X}_{RD-WDT}$ using the data of windward, leeward slopes and the combined data from two aspects[a]

	Ww				Lw			
	θ	u^*	$\bar{X}_{RD-WDT}$	*N*	θ	u^*	$\bar{X}_{RD-WDT}$	*N*
θ	1·0000 (0·0000)	0·0000 (1·0000)	0·0967 (0·5747)	36	1·0000 (0·0000)	0·0000 (1·0000)	0·0481 (0·7804)	36
u^*		1·0000 (0·0000)	0·9390 (0·0001)	36		1·0000 (0·0000)	0·8913 (0·0001)	36

Note: Ww, windward slope; Lw, leeward slope; u^*, wind shear velocity (in m s^{-1}); θ, slope gradient (deg); *N*, the number of data.
[a] The values of u^* are 0·53, 0·65, and 0·76 m s^{-1} at the Ww slopes and 0·34, 0·52, and 0·62 m s^{-1} at the Lw slopes for the horizontal wind velocities (u) of 6·4, 10·0, and 12·0 m s^{-1}, respectively.

DOI: 10.1002/esp

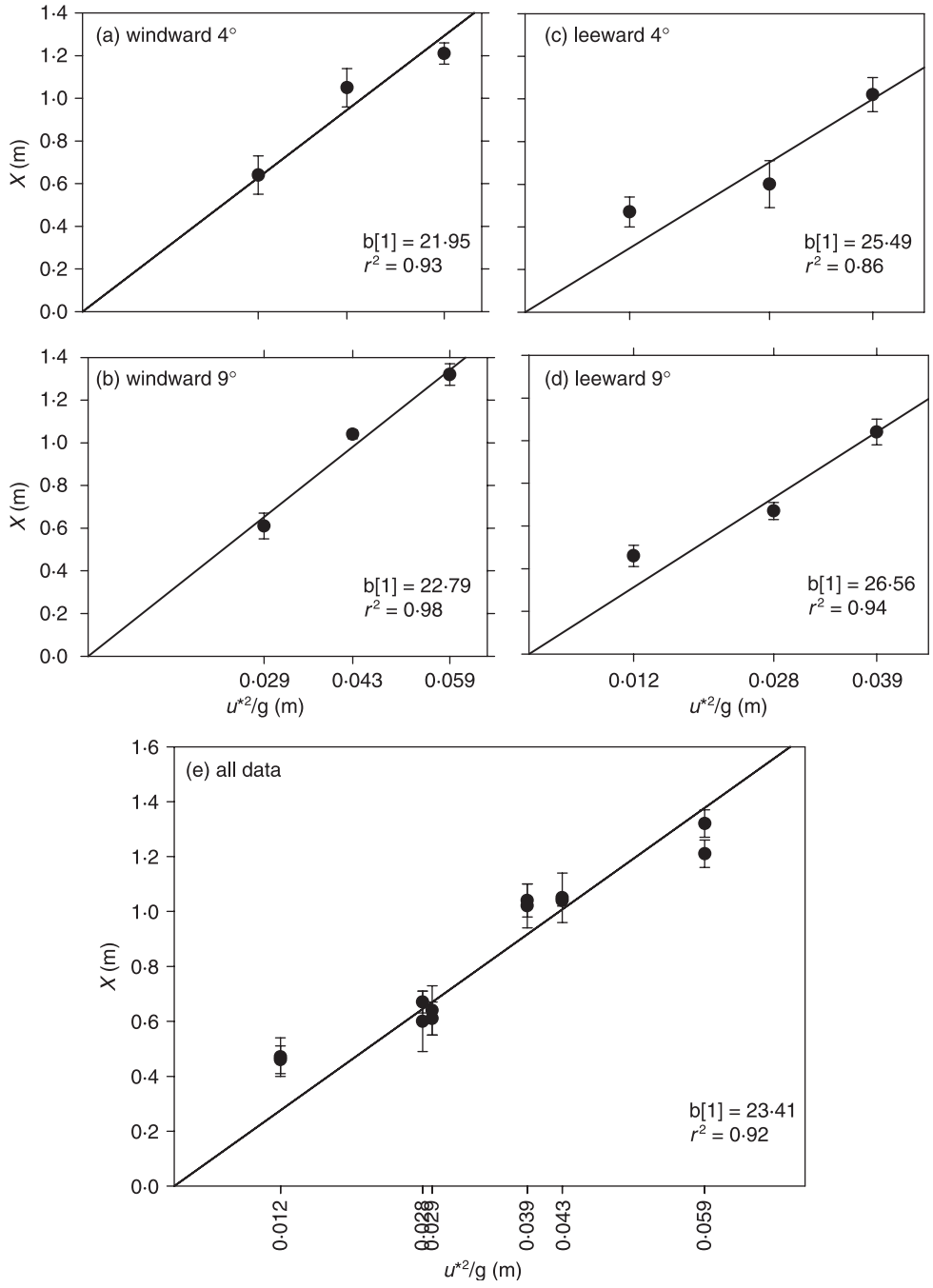

Figure 4. Linear regression models with $b_0 = 0$ for predicting $\bar{X}_{RD-WDT}$ by u^{*2}/g for the windward (a and b) and leeward slopes (c and d) of 4 and 9° and for full data irrespective of the slope aspect (e).

However, Cruse *et al.* (2000) reported that the relative importance of compressive and shear forces in soil detachment was vague.

At this point there emerge two significant differences between the splash phenomena of windless and wind-driven rains. Firstly, the shear forces that cause the particles to lift off with an initial velocity are associated directly with the compressive forces in the RD-ST process, which relies on the compensatory lateral jet development by the compressive pressure build-up at the raindrop–soil interface, although they are a function of u^* rather than the compressive forces in the RD-WDT process (Erpul *et al.*, 2005; Erpul *et al.*, 2008a, 2008b). Secondly, as it is previously stated statistically, the direction and magnitude of the splash asymmetry is independent of θ, and either upslope or downslope transport of grains occurs by the RD-WDT process, depending upon the prevailing wind direction (Erpul, 2001; Erpul *et al.*, 2002, 2004; Visser and Sterk, 2007). Therefore, the induced lateral jets by the horizontal wind velocity caused a longer travel path in the RD-WDT process than that of the RD-ST process resulting principally from the compensatory lateral jets produced by the compressive pressure build-up at the raindrop–sand surface.

However, Bagnold (1941) estimated the initial vertical velocity of particle lift-off to be of the order of u^*, and the force of transporting particles was expressed with u^*.

$$\tau_w = \rho_a u^{*2} \tag{5}$$

where τ_w is wind shear stress and ρ_a is air density. If τ_w is compared to that of the improved lateral jets of raindrops induced by horizontal wind (Equation 6), it is not unexpected that $\bar{X}_{WE-ST}$ is 2·27 times less than $\bar{X}_{RD-WDT}$.

$$\tau_{dss} = \rho_d V_x^2 \tag{6}$$

DOI: 10.1002/esp

where τ_{dss} is shear stress of the wind-driven raindrop, ρ_d is raindrop density, and v_x is raindrop horizontal velocity induced by wind. From these results of the current study, it is clear that the ejection velocity of the splash droplets caused by the wind-driven raindrop impact was greater not only than that of the splash droplets by the vertically impacting raindrops of windless rain but also than that of the particles by rolling or saltating grain colliding with the rainless wind.

Conclusions

This study demonstrated that average trajectory ($\bar{X}_{RD-WDT}$) of the RD-WDT process was not only different from the average trajectory of the windless rain process ($\bar{X}_{RD-ST}$), but also about $2{\cdot}27 \pm 2{\cdot}2$ times greater than the trajectory of a typical saltating sand particle of the rainless wind ($\bar{X}_{WE-ST}$). The RD-WDT mechanism might have such a considerable operational extent that it can considerably produce higher net downwind sediment transport when compared to those of both RD-ST and WE-ST.

References

Al-Durrah MM, Bradford JM. 1982. The mechanism of raindrop splash on soil surfaces. *Soil Science Society of American Journal* **46**: 1086–1090.

Bagnold RA. 1941. *The Physics of Blown Sand and Desert Dunes*. Methuen: London; 256 pp.

Blocken B, Carmeliet J. 2000. Driving rain on building envelopes – I: numerical estimation and full-scale experimental verification. *Journal of Thermal Envelope and Building Science* **24**: 61–85.

Blocken B, Carmeliet J. 2002. Spatial and temporal distribution of driving rain on a low-rise building. *Wind and Structures* **5**: 441–462.

Blocken B, Carmeliet J. 2004. A review of wind-driven rain research in building science. *Journal of Wind Engineering and Industrial Aerodynamics* **92**: 1079–1130.

Blocken B, Carmeliet J, Poesen J. 2005. Numerical simulation of the winddriven rain distribution over smallscale topography in space and time. *Journal of Hydrology* **315**: 252–273.

Blocken B, Poesen J, Carmeliet J. 2006. Impact of wind on the spatial distribution of rain over micro-scale topography – numerical modelling and experimental verification. *Hydrological Processes* **20**: 345–368.

Cornelis W, Erpul G, Gabriels D. 2004a. The I.C.E. wind tunnel for wind and water interaction research. In *Wind and Rain Interaction in Erosion*, Visser S, Cornelis W (eds), Tropical Resource Management Papers, Chapter 13. Wageningen University and Research Centre: Wageningen; 195–224.

Cornelis WM, Oltenfreiter G, Gabriels D, Hartmann R. 2004b. Splash–saltation of sand due to wind-driven rain: vertical deposition flux and sediment transport rate. *Soil Science Society of America Journal* **68**: 32–40.

Cornelis WM, Oltenfreiter G, Gabriels D, Hartmann R. 2004c. Splash-saltation of sand due to wind-driven rain: horizontal flux and sediment transport rate. *Soil Science Society of America Journal* **68**: 41–46.

Cruse RM, Berghoefer BE, Mize CW, Ghaffarzadeh M. 2000. Water drop impact angle and soybean protein amendment effects on soil detachment. *Soil Science Society of America Journal* **64**: 1474–1478.

De Lima JLMP. 1989. Raindrop splash anisotropy: slope, wind, and overland flow velocity effects. *Soil Technology* **2**: 71–78.

De Lima JLMP. 1990. The effect of oblique rain on inclined surfaces: a nomograph for the rain-gauge correction factor. *Journal of Hydrology* **115**: 407–412.

De Lima JLMP, Van Dijk PM, Spaan WP. 1992. Splash-saltation transport under wind-driven rain. *Soil Technology* **5**: 151–166.

De Ploey J. 1980. Some field measurements and experimental data on wind-blown sands. In *Assessment of Erosion*, De Boodt M, Gabriels D (eds). Wiley: Chichester; 143–151.

Ellison WD. 1947. Soil erosion studies. *Agricultural Engineering* **28**: (7 parts) 145–146; 197–201; 245–248; 297–300; 349–351; 407–408; 447–450.

Erpul G. 1996. *Determination of Rainfall Characteristics in a Wind Tunnel*, MSc Thesis, Ghent University; 106 pp.

Erpul G. 2001. *Detachment and Sediment Transport from Interrill Areas Under Wind-driven Rains*, PhD Thesis, Purdue University, West Lafayette, IN.

Erpul G, Gabriels D. 2006. Works on erosion processes under wind-driven rain conditions in I.C.E. In *New Waves in Physical Land Resources*, Longouche D, Van Rast E (eds), Proceedings of the Workshop for Alumni of the MSc Programmes in Soil Science, Eremology and Physical Land Resources, Ghent University, Ghent, 3–9 September; 24–34.

Erpul G, Gabriels D, Janssens D. 1998. Assessing the drop size distribution of simulated rainfall in a wind tunnel. *Soil and Tillage Research* **45**: 455–463.

Erpul G, Gabriels D, Janssens D. 2000. The effect of wind on size and energy of small simulated raindrops: a wind tunnel study. *International Agrophysics* **14**: 1–7.

Erpul G, Gabriels D, Norton LD. 2005. Sand detachment by wind-driven raindrops. *Earth Surface Processes and Landforms* **30**: 241–250.

Erpul G, Norton LD, Gabriels D. 2002. Raindrop-induced and wind-driven soil particle transport. *Catena* **47**: 227–243.

Erpul G, Norton LD, Gabriels D. 2003a. The effect of wind on raindrop impact and rainsplash detachment. *Transactions of the ASAE* **45**: 51–62.

Erpul G, Norton LD, Gabriels D. 2003b. Sediment transport from interill areas under wind-driven rain. *Journal of Hydrology* **276**: 184–197.

Erpul G, Norton LD, Gabriels D. 2004. Splash-saltation trajectories of soil particles under wind-driven rain. *Geomorphology* **59**: 31–42.

Erpul G, Gabriels D, Cornelis WM, Samray HN, Guzelordu T. 2008a. Sand detachment under rains with varying angle of incidence. *Catena* **72**: 413–422.

Erpul G, Gabriels D, Cornelis WM, Samray H, Guzelordu T. 2008b. Sand transport under increased lateral jetting of raindrops induced by wind. *Geomorphology*. DOI: 10.1016/j.geomorph.2008.08.012

Evans MG, Warburton J. 2005. Sediment budget for an eroding peat moorland catchment in Northern England. *Earth Surface Processes and Landforms* **30**: 557–577.

Foulds SA, Warburton J. 2007a. Wind erosion of blanket peat during a short period of surface desiccation (North Pennines, Northern England). *Earth Surface Processes and Landforms* **32**: 481–488.

Foulds SA, Warburton J. 2007b. Significance of wind-driven rain (wind-splash) in the erosion of blanket peat. *Geomorphology* **83**: 183–192.

Furbish DJ, Hamner KK, Schmeeckle M, Borosund MN, Mudd SM. 2007. Rainsplash of dry sand revealed by high-speed imaging and sticky paper splash targets. *Journal of Geophysical Research-Earth Surface* **112**: F1. DOI: 10.1029/2006JF000498

Gabriels D, Cornelis W, Pollet I, Van Coillie T, Quessar M. 1997. The I.C.E. wind tunnel for wind and water erosion studies. *Soil Technology* **10**: 1–8.

Gillette D. 1977. Fine particulate emissions due to wind erosion. *Transactions of the ASAE* **20**: 890–987.

Gilley JE, Finkner SC. 1985. Estimating soil detachment caused by raindrop impact. *Transactions of the ASAE* **28**: 140–146.

Gilley JE, Woolhiser DA, McWhorter DB. 1985. Interrill soil erosion. Part I: Development of model equations. *Transactions of the ASAE* **28**: 147–153, 159.

Goossens D, Poesen J, Gross J, Spaan W. 2000. Splash drift on light sandy soils: a field experiment. *Agronomie* **20**: 271–282.

Greeley R, Iversen JD. 1985. *Wind as a Geological Process on Earth, Mars, Venus and Titan*. Cambridge University Press: New York.

Grosh JL, Jarrett AR. 1994. Interrill erosion and runoff on very steep slopes. *Transaction of ASAE* **37**: 1127–1133.

Heymann FJ. 1967. A survey of clues to the relation between erosion rate and impact parameters. *Second Rain Erosion Conference* **2**: 683–760.

Huang C, Bradford JM, Cushman JH. 1982. A numerical study of raindrop impact phenomena: the rigid case. *Soil Science Society of America Journal* **46**: 14–19.

Huang C, Bradford JM, Cushman JH. 1983. A numerical study of raindrop impact phenomena: the elastic deformation case. *Soil Science Society of America Journal* **47**: 855–866.

Jungerius PD, Dekker LW. 1990. Water erosion in the dunes. *Catena* **18**(Suppl.): 185–193.

Jungerius PD, Verheggen AJT, Wiggers AJ. 1981. The development of blowouts in 'De Blink', a coastal dune area near Noordwijkerhout, the Netherlands. *Earth Surface Processes and Landforms* **6**: 375–396.

Kinnell PIA. 1999. Discussion on 'The European Soil Erosion Model' (EUROSEM): a dynamic approach for predicting sediment transport from fields and small catchments. *Earth Surface Processes and Landforms* **24**: 563–565.

Kinnell PIA. 2005. Raindrop-impact-induced erosion processes and prediction: a review. *Hydrological Processes* **19**: 2815–2844.

Legout C, Legue'dois S, Le Bissonnais Y, Issa OM. 2005. Splash distance and size distributions for various soils. *Geoderma* **124**: 279–292.

Legue'dois S, Planchon O, Legout C, Le Bissonnais Y. 2005. Splash projection distance for aggregated soils: theory and experiment. *Soil Science Society of America Journal* **69**: 30–37.

Moeyersons J. 1983. Measurements of splash-saltation fluxes under oblique rain. *Catena* **4**(Suppl.): 19–31.

Moeyersons J, De Ploey L. 1976. Quantitative data on splash erosion, simulated on unvegetated slopes. *Zeitschrift fur Geomorphologie* **25**(Suppl.): 120–131.

Morgan RPC. 2007. Field studies of rainsplash erosion. *Earth Surface Processes and Landforms* **3**: 295–299.

Mouzai L, Bouhadef M. 2003. Water drop erosivity: effects on soil splash. *Journal of Hydraulic Research* **42**: 61–68.

Nearing MA, Bradford JM, Holtz RD. 1986. Measurement of force vs. time relations for waterdrop impact. *Soil Science Society of America Journal* **50**: 1532–1536.

Owen PR. 1980. *Sand Movement Mechanism*. Workshop on Physics of Desertification. International Center for Theoretical Physics, Trieste, Italy.

Pedersen HS, Hasholt B. 1995. Influence of wind speed on rainsplash erosion. *Catena* **24**: 39–54.

Poesen J. 1985. An improved splash transport model. *Zeitschrift fur Geomorphologie N.F.* **29**: 193–221.

Poesen J. 1986. Field measurements of splash erosion to validate a splash transport model. *Zeitschrift fur Geomorphologie N.F.* **58**(Suppl.): 81–91.

Poesen J, Savat J. 1981. Detachment and transportation of loose sediments by raindrop splash. Part II: Detachability and transportability measurements. *Catena* **8**: 19–41.

Quansah C. 1981. The effect of soil type, slope, rain intensity and their interactions on splash detachment and transport. *Journal of Soil Science* **32**: 215–224.

Raupach MR, Lu H. 2004. Representation of land-surface processes in aeolian transport models. *Environmental Modelling and Software* **19**: 93–112.

Riezebos HT, Epema GF. 1985. Drop shape and erosivity. Part II. Splash detachment, transport and erosivity indices. *Earth Surface Processes and Landforms* **10**: 69–74.

Rutin J. 1983. *Erosional Processes on a Coastal Sand Dune, De Blink, Noordwijkerhout*. Laboratory of Physical Geography and Soil Science, University of Amsterdam: Amsterdam.

SAS. 1995. *SAS System for Elementary Statistical Analysis*. SAS Institute: Cary, NC; 280–285.

Savat J, Poesen J. 1981. Detachment and transportation of loose sediments by raindrop splash. Part I: The calculation of absolute data on detachability and transportability. *Catena* **8**: 1–18.

Shao Y, Raupach MR, Findlater PA. 1993. The effect of saltation bombardment on the entrainment of dust by wind. *Journal of Geophysical Research* **98**: 12719–12726.

Sharma PP, Gupta SC. 1989. Sand detachment by single raindrops of varying kinetic energy and momentum. *Soil Science Society of America Journal* **53**: 1005–1010.

Sharon D. 1970. Topography-conditioned variations in rainfall as related to the runoff contributing areas in a small watershed. *Israel Journal of Earth-Sciences* **19**: 85–89.

Sharon D. 1980. The distribution of hydrologically effective rainfall incident on sloping ground. *Journal of Hydrology* **46**: 165–188.

Sharon D, Arazi A. 1997. The distribution of wind-driven rain in a small valley: an empirical basis for numerical model verification. *Journal of Hydrology* **201**: 21–48.

Sharon D, Adar E, Lieberman G. 1983. Observations on the differential hydrological and/or erosional response of opposite-lying slopes, as related to incident rainfall. *Israel Journal of Earth-Sciences* **32**: 71–74.

Sharon D, Morin J, Moshe Y. 1988. Micro-topographical variations of rainfall incident on ridges of a cultivated field. *Transactions of the ASAE* **31**: 1715–1722.

Springer GS. 1976. *Erosion by Liquid Impact*. Wiley: New York.

Van Dijk AIJM, Meesters AGCA, Bruijnzeel LA. 2002. Exponential distribution theory and the interpretation of splash detachment and transport experiments. *Soil Science Society of America Journal* **66**: 1466–1474.

Van Dijk PM, Stroosnijder L, De Lima JLMP. 1996. The influence of rainfall on transport of beach sand by wind. *Earth Surface Processes and Landforms* **21**: 341–352.

Vieira G, Mora C, Gouveia MM. 2004. Oblique rainfall and contemporary geomorphological dynamics (Serra da Estrela, Portugal). *Hydrological Processes* **18**: 807–824.

Visser SM, Palma J. 2004. Up-scaling wind and water erosion models far from reality. In *Wind and Rain Interaction in Erosion*, Visser S, Cornelis W (eds), Tropical Resource Management Papers, Chapter 4. Wageningen University and Research Centre: Wageningen; 59–67.

Visser SM, Sterk G. 2007. Nutrient dynamics – wind and water erosion at the village scale in the Sahel. *Land Degradation* and *Development* **18**: 578–588.

Warburton J. 2003. Wind-splash erosion of bare peat on UK upland moorlands. *Catena* **52**: 191–207.

White BR, Schulz JC. 1977. Magnus effect on saltation. *Journal of Fluid Mechanics* **81**: 497–512.

Wright AC. 1986. A physically-based model of the dispersion of splash droplets ejected from a water drop impact. *Earth Surface Processes and Landforms* **11**: 351–367.

Wright AC. 1987. A method of the redistribution of disaggregated soil particles by rainsplash. *Earth Surface Processes Landforms* **12**: 583–596.

DOI: 10.1002/esp